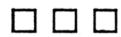


# EXTREME ULTRAVIOLET ASTRONOMY

A SELECTION OF  
PAPERS PRESENTED AT THE  
FIRST BERKELEY COLLOQUIUM ON  
EXTREME ULTRAVIOLET ASTRONOMY

University of California, Berkeley  
January 19–20, 1989



Co-Sponsored by  
IAU Commissions 29, 44, and 48

EDITED BY

ROGER F. MALINA  
Center for EUV Astrophysics  
University of California, Berkeley

STUART BOWYER  
Astronomy Department and  
Center for EUV Astrophysics  
University of California, Berkeley

**PERGAMON PRESS**

Member of Maxwell Macmillan Pergamon Publishing Corporation  
New York • Oxford • Beijing • Frankfurt  
Sao Paulo • Tokyo • Toronto

# EUV EXCESSES IN QUASARS

MARTIN ELVIS  
JONATHAN C. MCDOWELL

BELINDA J. WILKES

---

## 1. EUV EXCESSES—ACCRETION DISK SIGNATURES?

At energies below  $\sim 0.3$  keV ( $\geq 44$  Å the “C-band”), many quasars and AGN show large excess flux over the extrapolations of their higher-energy power laws (Wilkes and Elvis 1987; Elvis 1988; Turner and Pounds 1989). In these objects a continuum shape more complex than a simple power law is required to explain the full EUV–X-ray continuum; in many cases at least two separate emission components are required (see section 5 below).

It has been suggested that EUV excesses are emitted from the inner edges of accretion disks (Arnaud et al. 1985; Bechtold et al. 1986; Czerny and Elvis 1987). In such a case their radiation comes to us from the innermost identifiable region of a quasar, and their spectral shapes can provide information on the peak temperature in the disk and hence determine the allowed values of the central mass and the accretion rate. If, however, the EUV radiation is the result of reprocessing, e.g., by a Comptonizing atmosphere, these constraints become limits. We would instead gain information (such as temperature and optical depth of a scattering region) on the region of reprocessing, which itself must be close to the quasar’s center (Czerny and Elvis 1987).

Whatever their origin, these EUV excesses are a new component of the quasar continuum and deserve careful investigation. Existing observations are crude, little better than a single “photometry” point with occasional multiple observations indicating variability. Observations in the 100 Å band may be especially valuable since the components are likely to be particularly strong at these wavelengths.

## 2. OTHER KINDS OF SOFT EXCESS

We should note here that there appears to be at least one, and perhaps as many as four, other kinds of “soft excess” in AGN and related objects. In hard X-ray selected samples of AGN, roughly half of the objects are heavily obscured (Lawrence and Elvis 1982) and exhibit large low-energy cutoffs in their spectra because of photoelectric absorption by intervening material. Some of these heavily cutoff objects also show excess flux at low energies above extrapolations of their cutoff spectra (Reichert et al. 1985), although not above extrapolations of the high-energy continuum with the cutoff removed. These excesses have been explained in three different ways, depending on their time variability: a “leaky absorber” (e.g., NGC4151, Holt et al. 1980; Reichert et al. 1985); a partially ionized “warm” absorber (MR2251–179, Halpern 1984; NGC7213, Halpern and Filippenko 1984; NGC7469, Turner and Pounds 1989;

NGC4151, Yaqoob, Warwick, and Pounds 1989); or extended hot gas in the zone of the optical emission line gas (NGC4151, Elvis, Briel, and Henry 1983; Pounds et al. 1986a; NGC7314, Turner 1987; Akn 120, Turner and Pounds 1989) for the cases where the 2–10 keV flux varies while the  $\sim 0.2$  keV flux remains constant. NGC4151 appears in all the categories because it is so bright and hence is observed many times with the best available signal-to-noise. The complexity of the SXR emission from NGC4151 suggests that high-resolution spectra will someday reveal rich information about the inner regions of AGN.

A fourth type of soft excess is seen in BL Lac objects. Early reports (e.g., Agrawal, Riegler, and Mushotzky 1979) suggested a spectral curvature steepening to low energies at  $\sim 1$ – $2$  keV, almost a decade higher in energy than the C-band excesses typical of emission-line AGN. The 0.5–3.5 keV spectra of BL Lacs most often appear to be power law extensions of their UV continua (Madejski and Schwartz 1988). More recent spectra (Barr, Giommi, and Maccagni 1988) indicate the opposite curvature (i.e., steepening to higher energies). The observational situation is presently somewhat confused.

We are concerned here only with those excesses found in the quasars and AGN that have no observable low-energy absorption in their X-ray spectra, beyond the unavoidable column density due to our Galaxy. Fortunately, such objects are easy to find.

### 3. COMMON AND PERSISTENT

EUV excesses in quasars are common. Table 1 lists the 25 cases known as of January 1989. Half of these were found without a major survey. The other half come from two surveys of AGN and quasar X-ray spectra, one using *EXOSAT* (Turner and Pounds 1989); the other, by our group, using the *Einstein* IPC (Wilkes and Elvis 1987; Masnou et al. 1989). Our survey finds that for a signal-to-noise ratio limited subset of IPC quasars (Wilkes and Elvis 1987),  $\sim 50\%$  (8 out of 14) show significant EUV excesses. Our threshold for detection of excesses is quite high, a factor of 3 excess at 0.2 keV ( $\sim 60$  Å) above the extrapolation of the 0.5–3 keV spectrum.

Many more quasars might have EUV excesses that are only slightly below this threshold. Figure 1 shows an example of an EUV excess in the context of the same quasar's optical and UV emission. Turner and Pounds (1989) find that of the 18 AGN in their sample without large column densities (i.e.,  $\leq 10^{21}$  atoms  $\text{cm}^{-2}$ ), nine showed excess flux in the 3 Lexan CMA filter ( $E_{\text{eff}} \sim 0.15$  keV,  $\sim 80$  Å) above an extrapolation of the ME 2–8 keV spectrum.

Source counts from the low-energy imager on *EXOSAT* also indicate a large number of EUV excesses (Branduardi-Raymont et al. 1985; Giommi and Tagliaferri 1987). The number of EUV excesses also becomes clear when a comparison with *Einstein's* "Medium Survey" source counts (Gioia et al. 1984) and mean spectra (Maccacaro et al. 1988) is considered. Typical spectral indices of *Einstein* IPC-selected AGN are  $\alpha_E \sim 1.0$  (Maccacaro et al. 1988). If this slope applied down to the  $\sim 0.15$  keV ( $\sim 80$  Å) energy of the *EXOSAT* CMA/3 Lexan combination, the strong interstellar absorption at these energies would allow very few extragalactic detections. Instead, many AGN are seen (Branduardi-Raymont et al. 1985; Giommi and Tagliaferri 1987). A mean slope for 0.05–2.0 keV of  $\sim 1.5$  is needed to explain this observation and, given the mean slope for 0.5–3.5 keV of 1.0, this implies a slope in the C-band ( $\sim 0.05$ – $0.28$  keV,  $\sim 250$ – $44$  Å) that is significantly steeper than 1.5.

These excesses are persistent features. Several have been seen during observations spanning several years. Mkn 335 showed a clear excess in six observations over the three-year life of the *EXOSAT* mission. The longest time span covered so far is a series of five *Einstein* and *EXOSAT* observations of PG1211+143 over seven years, from a "pre-discovery" serendipitous *Einstein* observation in 1979 to a late *EXOSAT* observation in 1986. All show a strong EUV excess (Elvis et al. 1989).

TABLE 1—EUV EXCESSES (REPORTED AS OF JANUARY 1989)

Quasar	Instrument	$N_{\text{H}}(\text{Gal})^a$	Variable?	References
PHL909	IPC	4.2		Masnou et al. 1989
MKN335	CMA		√	Pounds et al. 1987; Lee et al. 1988; Turner and Pounds 1988, 1989
F-9	CMA	2.3 <sup>b</sup>		Morini et al. 1986, Turner and Pounds 1989
NAB0205+024	IPC	3.0		Masnou et al. 1989
NGC1068	CMA, IPC	3.1		Monier and Halpern 1987; Elvis and Lawrence 1988
AKN120	CMA	9.7 <sup>c</sup>		Turner and Pounds 1989
NGC2110	CMA	18.6		Turner and Pounds 1989
M81	IPC	4.1 <sup>c</sup>	√	Fabbiano 1988
NGC4051	CMA	1.3	√	Marshall et al. 1983; Lawrence et al. 1985, 1987; Turner and Pounds 1989
3C273	CMA, IPC	1.8 <sup>d</sup>		Turner and Pounds 1989; Masnou 1989
PG1211+143	IPC	2.8	√	Elvis, Wilkes, and Tananbaum 1985; Bechtold et al. 1987; Masnou et al. 1989; Elvis, Lockman, and Wilkes 1989
MKN205	IPC	4.3		Masnou et al. 1989
NGC4593	CMA	2.0		Turner and Pounds 1989
MCG-6-30-15	CMA	4.1		Turner and Pounds 1989
NGC5548	CMA	1.7 <sup>c</sup>		Branduardi-Raymont et al. 1985; Turner and Pounds 1989
PG1426+015	IPC	2.6		Masnou et al. 1989
MKN841	CMA	2.2	√	Arnaud et al. 1985; Fabian et al. 1986
E1615+061	HEAO-A2	4.6 <sup>c</sup>	√ <sup>e</sup>	Pravdo and Marshall 1984; Piro et al. 1988
MCG-2-58-22	CMA	3.5 <sup>c</sup>		Morini et al. 1987
MKN509	HEAO-A2	5.6 <sup>c</sup>	√	Singh, Garmire, and Nousek 1985
	CMA			Morini et al. 1987
IIZw136	IPC	4.2		Masnou et al. 1989
NGC7213	CMA, IPC	1.6 <sup>b</sup>		Halpern and Fillipenko 1984; Turner and Pounds 1989
NGC7314	CMA	1.5		Turner and Pounds 1989
MR2251-179	CMA	2.8		Turner and Pounds 1989
NGC7469	CMA <sup>f</sup>	4.8		Barr 1986; Turner and Pounds 1989

<sup>a</sup>  $10^{20} \text{ cm}^{-2}$ , Elvis, Lockman, and Wilkes (1989), ( $\pm 1 \times 10^{19} \text{ cm}^{-2}$ ).

<sup>b</sup> Too southern for Green Bank.  $N_{\text{H}}$  from Heiles and Cleary (1979).

<sup>c</sup>  $N_{\text{H}}$  from Bell Labs survey, Stark et al. 1984, ( $\pm 1 \times 10^{20} \text{ cm}^{-2}$ ).

<sup>d</sup>  $N_{\text{H}}$  from Arecibo emission/absorption measurement (Dickey, Salpeter, and Terzian 1978).

<sup>e</sup> It is possible that the original, large-beam, HEAO-A2 detection was confused by the strong RSCVn star in the field (Buckley et al. 1987), so no EUV excess was present.

<sup>f</sup> Excess low-energy flux may be due to a partially ionized absorber.

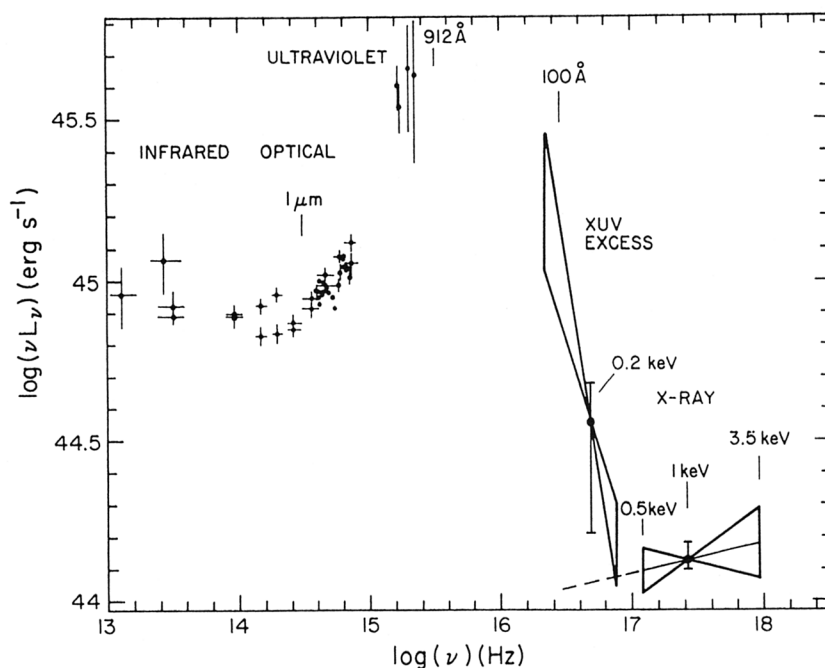


FIGURE 1—Infrared to X-ray spectrum of PG1426+015 (MKN 1383) a quasar with an EUV excess. The “bow-tie” shape on the right shows the allowed range (at 90% confidence) of power laws that can be fitted to the 0.5–3.5 keV *Einstein* IPC data. The data point to the left of this shows the strength of the EUV excess at 0.2 keV (62 Å) that is needed to explain the “ $N_H$ ” value given by the spectral fit. A second bow-tie showing power law slopes  $2.5 < \alpha_E < 3.5$  in the 0.1–0.28 keV (120–44 Å) region. The lower end of this bow-tie is near the 100 Å band of *EUVE* and the *ROSAT* WFC.

A somewhat different case is that of NGC1068, a type 2 (i.e., narrow-lined) Seyfert galaxy. NGC1068 also showed a soft excess in 1979 *Einstein* observations (Monier and Halpern 1987) that was present at the same level in *EXOSAT* observations in 1983 and 1985 (Elvis and Lawrence 1988). The lack of variability in this soft excess is unusual (see section 4) and adds weight to the idea that the X-rays, along with the optical nonthermal continuum and the polarized, broad emission lines are seen not directly but only after scattering of a warm plasma (Antonucci and Miller 1985; Elvis and Lawrence 1988).

#### 4. VARIABLE, OPTICALLY THICK

EUV excesses, however, vary rapidly by quite large factors. A large fraction (7 out of 25) of the UV excess components in Table 1 have been seen to vary even though most of them have been observed only a few times. The deep CMA survey of the Coma region (Branduardi-Raymont et al. 1985) is particularly striking. In two observations separated by two years, three of the five AGN changed their flux by at least a factor of 2. (These CMA fluxes must be dominated by the steep EUV component in order to be detectable; see above). This behavior contrasts with the relative lack of variability in the  $\sim 0.5$ –3 keV band of the IPC (Zamorani et al. 1984) and in the higher energy ( $\sim 2$ –20 keV) band of traditional collimated proportional counters (in particular *HEAO-A2*, Tennant and Mushotzky 1983).

Variability time scales down to days (Elvis et al. 1989) and even hours (Turner and Pounds 1988; Lee et al. 1988) have been seen involving flux changes of order a factor of 2. Rapid changes like this trivially rule out the presence of extended regions of emission on the scale of the optical-UV emission line cloud zones ( $\sim 1$  pc to 1 kpc). Hot confining media had been suggested to contain both the broad (Krolik, McKee, and Tarter 1981) and narrow (Halpern and Filippenko 1984) emission line clouds and so are a reasonable source of SXR. However, they do not appear to be the dominant source of SXR in most quasars.

Rapid decreases in flux also rule out a more general class of models, optically thin thermal emission from a hot plasma, e.g., in a corona above an accretion disk. If the EUV excesses were due to an optically thin thermal plasma, then their spectra would be rich in diagnostic emission lines and would be a treasure trove of information on the centers of quasars. Unfortunately, we show below that this situation is unlikely (Elvis et al. 1989).

The cooling times for such a gas, even assuming the largest possible size from the light travel time, are easily rapid enough to produce the observed decreases in flux. The maximum radius,  $R$  (cm), of a uniform sphere of plasma at temperature  $T$  (K), that can cool in a time,  $t$  (days), is given by

$$R = 4.7 \times 10^{16} (L_{45} f t^2)^{1.3} T_6^2,$$

for a luminosity  $L_{45}$  ( $10^{45}$  erg  $s^{-1}$ ) and where  $f$  is a factor ( $0.2 < f < 8$ ) that allows for the variation of cooling by line emission (Mewe and Gronenschild 1981). For the case of PG1211+143 (Elvis et al. 1989), this gives a radius of  $5 \times 10^{18}$  cm, which is ten times larger than the light-crossing time constraint. A smaller sphere will cool faster, so there is no problem with thermally cooling the plasma.

However, if we take the implied size from the light travel time and calculate the optical depth to electron scattering through the hypothetical sphere of emitting gas, we find that it is large. The density,  $n_e$  ( $cm^{-3}$ ), of the plasma is given by

$$n_e = 4.8 \times 10^8 f^{-1} T_6 t,$$

and the optical depth to electron scattering ( $\tau_{es}$ ) is given by

$$\tau_{es} = n_e R \sigma_{es},$$

where  $\sigma_{es}$  is the Thomson cross section. For the PG1211+143 example, the plasma is far from optically thin since  $\tau_{es} \geq 200$ , for a 190 light-day size. Smaller sizes increase  $\tau$  as  $R^{1/2}$ . Optically thin, line-emitting gas is thus ruled out as the dominant source of luminosity for the variable EUV excesses.

## 5. STEEP SPECTRA

The low-energy spectra do not constrain well the spectral shapes of the EUV excesses. Masnou et al. (1989) took the combined *Einstein* IPC and MPC data for the best signal-to-noise ratio quasars. If accurate galactic  $N_H$  values are used also (Elvis, Lockman, and Wilkes 1989), they can constrain the spectral shapes of these excesses. Two-component spectral fits require EUV power law energy indices at least as steep as 2.0, or black-body temperatures of  $\leq 0.2$  keV. Figure 1 shows these slopes for one example quasar.

Turner and Pounds (1989) fitted two-power laws to six AGN with EUV excesses using the three main *EXOSAT* filters (thin Lexan, aluminum, and boron) together with the ME (2–8 keV) data. These fits also require steep EUV slopes of  $\geq 2.5$ , and in one case  $\geq 4.5$  (MCG-

6–30–15). This general steepness is supported by the hint that the excesses are less commonly observed for quasars at redshifts  $\geq 0.2$  (Masnou et al. 1989), which would suggest that the onset of the excess is quite sudden, thus implying a steep spectrum.

## 6. CONNECTION TO THE REST OF THE QUASAR CONTINUUM?

How do the EUV excesses relate to the other components of the quasar continuum? We might in particular expect close links to the neighboring X-ray and UV regions.

On the X-ray side, the increase of variability as the energy of the X-ray observations decreases (see section 4) has been seen in individual objects (e.g., Turner and Pounds 1988; Elvis et al. 1989). The increased variability indicates that the EUV excess is indeed a separate component of the continuum, only weakly linked to the harder X-ray emission. Another possible link would be to the slope of the higher energy spectrum. The radio-loudness of a quasar is the main parameter determining the  $\sim 0.5$ – $3.5$  keV spectral slope (Wilkes and Elvis 1987). Radio-loudness, however, does not affect the chance of seeing an EUV bump (Masnou et al. 1989).

The UV connection initially appeared more promising. Wilkes and Elvis (1987) noted that the BL Lacs studied with the IPC give good fits to the galactic  $N_{\text{H}}$  in contrast to the subgalactic  $N_{\text{H}}$  values that the quasars typically gave. It appears that BL Lacs do not show the EUV excesses of the emission line objects, just as they do not show the optical-UV “big bump.” A link between the big bump and the EUV excess is an obvious suggestion and was the cause of the speculation on accretion disk models. However, no correlation of the presence of an excess with the strength of the optical-UV big bump in individual quasars shows up in the study by Masnou et al. (1989).

This is somewhat puzzling and frustrating. One possibility is that the lack of correlations found so far simply reflects the small dynamic range of EUV excesses detectable in the present data.

## 7. VISIBLE AT 100 Å?

An extrapolation of this steep slope to the 100 Å EUV band of *EUVE* or the *ROSAT* WFC is highly uncertain, given the poor quality of the existing spectra, but gives values some 40 times brighter than are given by extrapolation of the higher-energy X-ray spectra. Figure 1 illustrates this extrapolation. It is clear from Figure 1 that this extrapolation brings the EUV flux to the same  $\nu f_{\nu}$  level as the UV. A much larger value than 40 times brighter is thus unlikely. (Accretion disk models that reach above this level also tend to be highly super-Eddington, Bechtold et al. 1987). A much lower value is also possible; indeed, disk atmospheric models can include a strong helium absorption edge that would greatly reduce the 100 Å flux.

To stand a good chance of seeing this EUV component at 100 Å, one needs to look toward quasars and AGN with exceptionally low values of galactic  $N_{\text{H}}$ . The objects in Table 1 have galactic column densities of at least  $1.3 \times 10^{20}$  atoms  $\text{cm}^{-2}$ , and more typically  $\sim 3 \times 10^{20}$  atoms  $\text{cm}^{-2}$ . These are normal values. In observing a sample of nearly 200 AGN and quasars, Elvis, Lockman, and Wilkes (1989) found two objects with  $N_{\text{H}}$  values of  $0.9 \times 10^{20}$  atoms  $\text{cm}^{-2}$  or less and seven with  $N_{\text{H}}$  values  $< 1.1 \times 10^{20}$  atoms  $\text{cm}^{-2}$ . Thus, only 1–4% of randomly chosen AGN will make good 100 Å targets.

Clearly, the choice of targets will take some care. At a column density of  $1 \times 10^{20}$  atoms  $\text{cm}^{-2}$ , the transmission at 60 Å (0.2 keV) is 0.42. At 100 Å (0.124 keV) it is 10 times smaller, 0.042 (Morrison and McCammon 1983). A power law index of 4.8 between

TABLE 2—LOW GALACTIC COLUMN DENSITY AGN

Quasar	R.A.		decl.		$N_{\text{H}} (\times 10^{20})$		$f_{\text{x}}(\text{IPC})^{\text{a}}$	
3C345	16	41	17.6	39	54	10	0.74	2.83
3C263	11	37	09.3	66	04	26	0.82	0.79
PG1630+377	16	30	15.1	37	44	11	0.90	—
NGC 5033	13	11	09.1	36	51	29	1.00 <sup>b</sup>	0.16
3C277.1	12	50	14.9	56	50	38	1.03	0.50
MKN 231	12	54	04.9	57	08	36	1.03 <sup>b</sup>	< 0.26 <sup>c</sup>
3C287	13	28	15.9	25	24	38	1.06	5.15

<sup>a</sup>  $10^{-12}$  erg  $\text{cm}^{-2}$   $\text{s}^{-1}$ , for  $\alpha = 1.0$ ,  $N_{\text{H}} = N_{\text{H}}(\text{Gal})$  in the standard *Einstein* IPC broad band (0.16–3.5 keV). Fluxes from the *Einstein* quasar catalog (Wilkes et al. 1989).

<sup>b</sup> Heavily absorbed optically.

<sup>c</sup> Kriss (1982), for 0.5–4.5 keV.

60 Å (0.2 keV) and 100 Å is needed to cancel out this increased absorption. Such slopes may well be present (see section 5), but clearly any additional column will require steeper slopes and will rapidly lead to undetectability, even when strong excesses are present. To help begin the selection process, in Table 2 we list the seven quasars from Elvis, Lockman, and Wilkes (1989) with  $N_{\text{H}} < 1.1 \times 10^{20}$  atoms  $\text{cm}^{-2}$ .

These quasars will be particularly good targets for 100 Å observations designed to limit the long wavelength flux of any EUV excesses. The only caution here is that the  $N_{\text{H}}$  values may be underestimates since extra-ionized hydrogen column may be present (Reynolds 1985, 1989) along with associated EUV absorbing, neutral helium. The implication would then be that the EUV excesses are stronger than we had estimated, but more difficult to detect at 100 Å. Only observations can tell.

*Acknowledgments.* We wish to thank our collaborators, especially P. Giommi, G. Zamorani, and J.-L. Masnou for their assistance in this work; T. J. Turner for useful discussions; and F. J. Lockman, D. McCammon, and R. Reynolds for valuable discussions on galactic column densities. This work was supported by NASA Astrophysics Data Program grant NAG8-689, by NASA contract NAS8-30751, and by Smithsonian Institution Research Opportunities funding.

*Martin Elvis, Belinda J. Wilkes, and Jonathan C. McDowell are at the Harvard-Smithsonian Center for Astrophysics, 60 Garden Street, Cambridge, MA 02138.*